

Mechanical Properties of Chalcogenide Optic Fiber Material Based Tellurium

M.M.El-zaidia , Z.H.El-Gohary, M.S.AboGhazala, G.M.Turky* and E.A.Rabea.

Phys.Dept. Faculty of science, Menoufia university shebin El.koom,Egypt *Microwave Physics & Dielectrics

Department, National Research Centre (NRC),Egypt. Corresponding Author: M.M.El-zaidia

Corresponding Author: M.M.El-zaidia

Abstract: The variation of microhardness of the samples of the system $Te_{80}S_{20-x}B_x$ where ($x=0,2.5,5$ and $B=In$ or As) with the applied test load depends on the sample structure. The sample $Te_{80}S_{20}$ is still elastic until the applied load exceed 2N. The addition of In or As on expense of S, leads to increase the elastic limit. Mayer index (n) of all samples is greater than two. This means that all samples are soft and follow the reverse indentation size effect (RISE). Using indentation induced cracking (IIC) model, ensure the generation of micro-cracks. The behavior of the calculated elastic moduli confirm these results.

Date of Submission: 13-02-2019

Date of acceptance: 28-02-2019

I. Introduction

The chalcogenide glasses are known as optical material around 50 years ago (1), due to its interesting properties such as a wide transparency range, low optical losses, stability to atmospheric moisture (2,3), high non-linearity of optical properties, etc. Due to these reasons, the chalcogenide glasses are first candidate for the production of optic fibers cables (4).

Tellurium-rich alloys are better transparency in the infrared region means these glasses are a good choice for optical devices (5-7). Chalcogenide glasses are insoluble in water, concentrated hydrochloric acid and its softer glass fibers than silica due to the two-fold coordinated chalcogen atoms. They behave as a flexible electron-lattice coupling system when they are subject to exhibit electro-atomic responses (8,9).

The micro-hardness of the glass depends on the atomic radius and the bulk density. The addition of tellurium to chalcogenide glasses improve its mechanical properties due to the increase of atomic mass and atomic radius (10).

The aim of the present research is to study the mechanical properties of the system $Te_{80}S_{20-x}B_x$ ($x=0,2.5,5$ and $B=In$ or As). The microhardness as a function of applied test load were recorded. The young modulus, yield strength, stiffness, fracture toughness and brittleness are also determined.

II. Experimental

The chalcogenide samples of the system $Te_{80}S_{20-x}B_x$ where ($x=0,2.5,5$ and $B=In$ or As) were prepared by melting quenching technique. Elements Se, S, Te, In & As were weighted and mixed well using the ball milling method for each sample alone. The homogeneous mixture was placed in an evacuated (10^{-4} Pa) and capsulated silica tube. The silica tube containing each sample was heated at fixed temperature for fixed time. The sample $Te_{80}S_{20}$ and the samples contain In on the expense of S were melted at 500C for 8 hours and quenching in ice water. The samples containing As on the expense of S were melted at 800C for 8 hours and then quenching in ice water. The microhardness of samples were investigated using Vicker's microhardness technique.

III. Result and discussion

The nonlinear variation of microhardness (H_v) as a function of the applied test load $F(N)$ for the system $Te_{80}S_{20-x}B_x$ where ($x=0,2.5,5$) and $B=In$ or As is shown in figure [1].

This behavior can be controlled by the relation (11)

$$H_v = 0.1891 \frac{F}{d^2}$$

Where H_v is Vicker microhardness in GPa, F is applied test load in Newton (N) and d is the arithmetic mean of the two diagonals (mm).

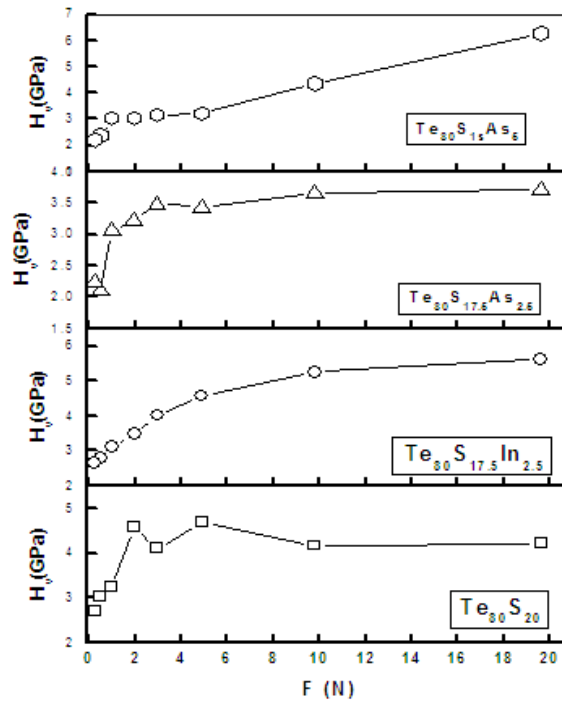


Fig [1] Vickers microhardness as a function of the applied test load for chalcogenide system $Te_{80}S_{20-x}B_x$ [where $x=0, 2.5, 5$ $B=In$ or As].

Fig [1] shows that, all samples are elastic till the applied test load exceeds the elastic limits. The elastic limit is differ from sample to sample. In case of the sample $Te_{80}S_{20}$, the elastic limit is 4N, this is corresponding the microhardness value 4.5GPa. As the applied test load exceeds 4N the sample surface suffers from some distortion around the indentation point. This may be due the generation of micro-cracks.

The factors affecting the microhardness as a function of the test load are interatomic bond length and bond energy strength. The values of possible bond length and bond energy strength were collected and tabulated in table [1]. Table [1] illustrate that the bond length and bond energy strength normally in inverse proportional to each other.

Table [1]

S.No.	Bond	Bond energy (KJ/mole)	Bond length Å
1	Te-Te	257.6	2.74
2	Te-S	335	2.405
3	Te-As	327	2.571
4	Te-In	215.5	2.81994
5	As-As	385.8	2.42
6	In-In	82	3.020
7	S-S	425.30	2.39
8	S-In	379.5	2.602
9	S-As	287.9	2.29

To understand the microhardness behavior well, the obtained results will be analyzed on the light of some models, as follow:

Mayer's law: -

Mayer's law illustrates the relation holding the applied test load $F(N)$ and diagonal of indentation (d) by equation (12),

$$F = Ad^n$$

Where n is Mayer exponent.

The value of n classify the behavior of microhardness H_v of any sample as follow:

- 1- If the value of (n) is more than the value two ($n>2$) the materials under test is soft and its microhardness follow the reverse indentation size effect (RISE).

- 2- If the value of (n) is less than the value two ($n < 2$) the materials under test is hard and its microhardness follow the indentation size effect (ISE).
- 3- If the value of (n) is equal to the value two ($n = 2$) the microhardness is independent on the applied load.

This can be carried out by drawing the relation ($\log F$) vis ($\log d$) for each sample of the system $Te_{80}S_{20-x}B_x$ where [($x=0, 2.5, 5$) and $B=In$ or As] as in fig [2]. The obtained values of n are collected in the table [2].

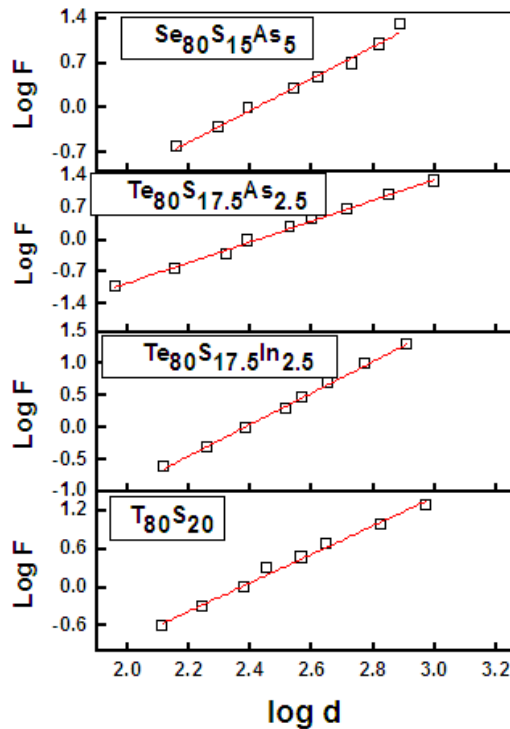


Fig [2] plot Log F and Log d of chalcogenide system $Te_{80}S_{20-x}B_x$ [where $x=0, 2.5, 5$ $B=In$ or As].

Table [2]

S.No.	Sample	Meyer's index(n)
1	$Te_{80}S_{20}$	2.23
2	$Te_{80}S_{17.5}In_{2.5}$	2.45
3	$Te_{80}S_{17.5}As_{2.5}$	2.26
4	$Te_{80}S_{15}As_5$	2.49

Table [2], illustrate that the values of n are greater than the value two ($n > 2$). This means that, the sample under test is soft and its microhardness follow reverse indentation size effect (RISE). The addition of In or As on the expense of S, leads to increase the elasticity. The elasticity was revealed to be more pronounced as As content reach 5 at %.

Indentation induced cracking (IIC) model

Indentation induced cracks IIC model (13) can be explained by drawing $\log (H_v)$ microhardness as a function of $\log (F^{5/3} / d^3)$ for the chalcogenide sample of the system $Te_{80}S_{20-x}B_x$ where ($x=0, 2.5, 5$) and $B=In$ or As shown in figure [3].

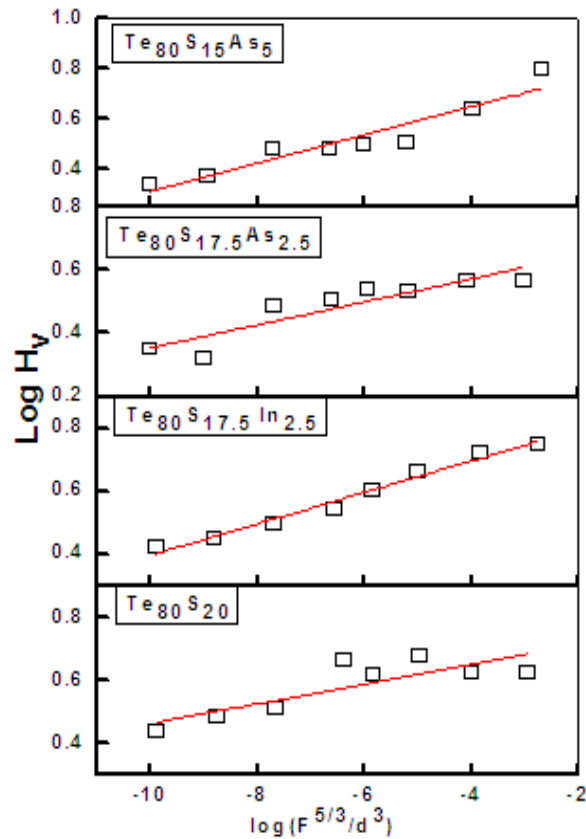


Fig [3] plot $\text{Log } H_v$ and $\log (F^{5/3}/d^3)$ for chalcogenide system $\text{Te}_{80}\text{S}_{20-x}\text{B}_x$ [where $x=0, 2.5, 5$ B=In or As]

Table [3]

S.No.	Sample	m
1	$\text{Te}_{80}\text{S}_{20}$	0.03126
2	$\text{Te}_{80}\text{S}_{17.5}\text{In}_{2.5}$	0.05008
3	$\text{Te}_{80}\text{S}_{17.5}\text{As}_{2.5}$	0.05582
4	$\text{Te}_{80}\text{S}_{15}\text{As}_5$	0.03654

Table [3] shows that the values of m is much less than 0.6. This means that the samples under test behaves as RISE.

Finally, the detected samples cracking were generated when the applied test load exceeds the elastic limit for each sample of the system $\text{Te}_{80}\text{S}_{20-x}\text{B}_x$ where [($x=0, 2.5, 5$) and B= In or As]. This elastic limit can be used as point of control during the manufacture of optic fiber from the chalcogenide system $\text{Te}_{80}\text{S}_{20-x}\text{B}_x$ where [($x=0, 2.5, 5$) and B= In or As].

The mechanical elastic moduli of the system $\text{Te}_{80}\text{S}_{20-x}\text{B}_x$

The obtained experimental resulted of the microhardness can be used to investigate the rest of the material mechanical moduli of the system $\text{Te}_{80}\text{S}_{20-x}\text{B}_x$ where [($x=0, 2.5, 5$) and B= In or As].

1- Young modulus(Y)

Fig [4] shows the linear relation of young modulus as a function of microhardness of the chalcogenide system $\text{Te}_{80}\text{S}_{20-x}\text{B}_x$ where [($x=0, 2.5, 5$) and B= In or As] (14).

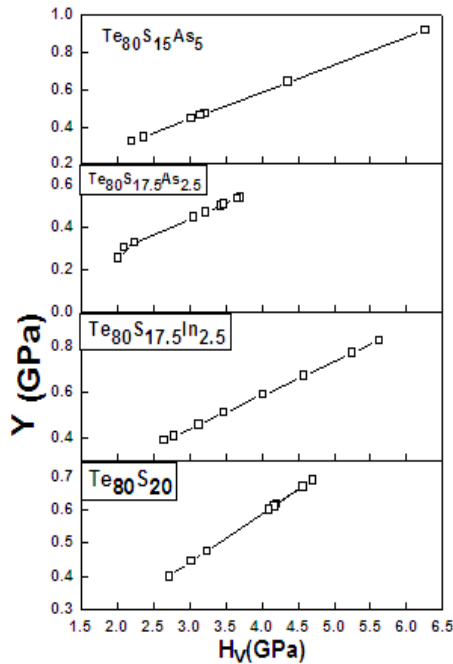


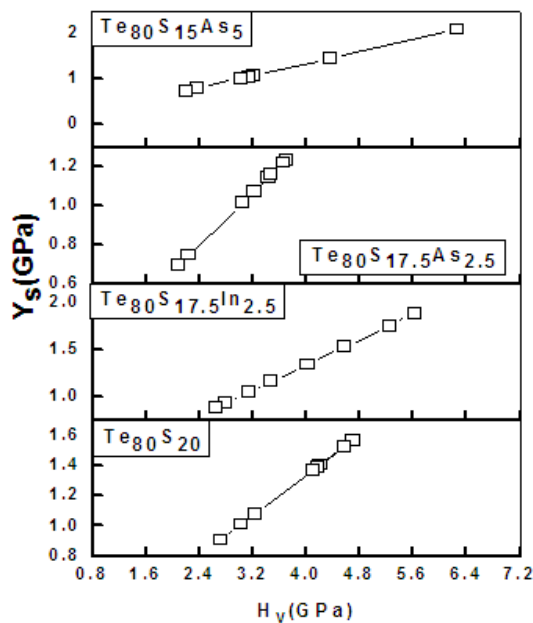
Fig [4] plot the young modulus Y as a function of microhardness (H_v) of the chalcogenide system Te₈₀S_{20-x}B_x [where x=0, 2.5, 5 B=In or As] .

Fig [4] proves that, the samples of the system Te₈₀S_{20-x}B_x where [(x=0, 2.5, 5) and B= In or As] are elastic. The addition of In or As on the expense of S , leads to increase the elasticity.

2- Yield strength (Y_s)

The linear variation of yield strength (Y_s) as a function of microhardness (H_v) is shown in fig [5] (15)

Fig [5] confirmed the elastic behavior of samples of the system Te₈₀S_{20-x}B_x where [(x=0, 2.5, 5) and B= In or As]. Also, fig [5] proves that the addition of In or As leads to increase elasticity of samples.



F2ig [5] plot the yield strength (Y_s) as a function of microhardness (H_v) of the chalcogenide system Te₈₀S_{20-x}B_x [where x=0, 2.5, 5 B=In or As] .

3- Stiffness constant (C_{II})

Fig [6] shows the relation between stiffness C_{II} and the microhardness of the samples of the system $Te_{80}S_{20-x}B_x$ where [(x=0,2.5,5) and B=In or As] (16).

Fig [6] proves that, the stiffness constant increases with microhardness. This means that, the deformation resistance of the sample increases as the applied test load increases.

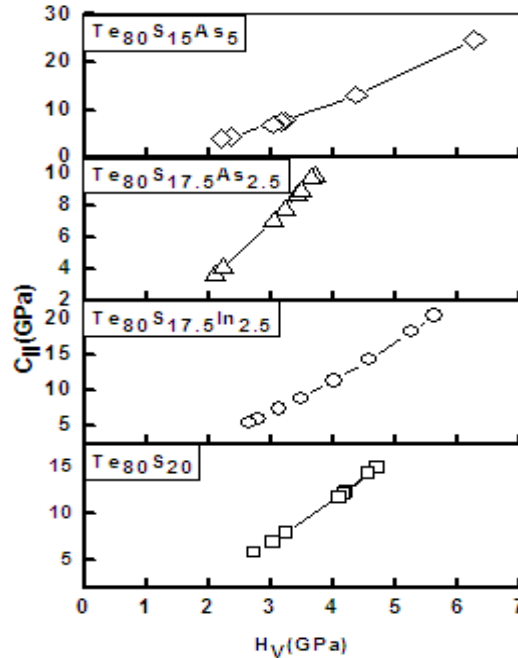


Fig [6] variation of stiffness(C_{II}) and with microhardness of the chalcogenide system $Se_{80}S_{20-x}B_x$ [where x=0, 2.5 ,5 B=In or AS].

4- Fracture toughness(K_F)

Fig [7] shows the variation of fracture toughness as a function of microhardness (H_v) of the system $Te_{80}S_{20-x}B_x$ where [(x=0 ,2.5 ,5) and B= In or As] (17).

Fig [7] proves that , the fracture toughness is decreased as microhardness increased. Also, The fracture toughness is decreased after the addition In or As.

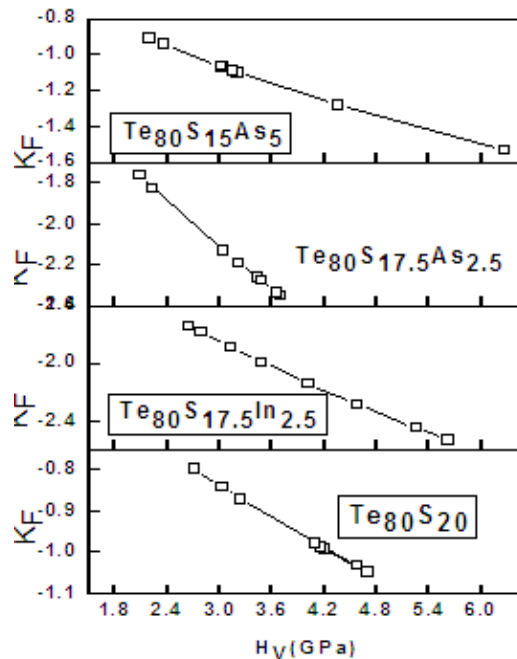


Fig [7] plot the fracture toughness (K_F) as a function of microhardness (H_v) of the chalcogenide system $Te_{80}S_{20-x}B_x$ [where x=0, 2.5 ,5 B=In or AS] .

5- Brittleness (B)

Fig [8] shows the brittleness(B) as a function of microhardness (H_v) of the chalcogenide system $Te_{80}S_{20-x}B_x$ [where $x=0, 2.5, 5$ B=In or AS] (16).

The brittleness of samples was decreased with the increasing of microhardness of the system $Te_{80}S_{20-x}B_x$ [where $x=0, 2.5, 5$ B=In or AS].

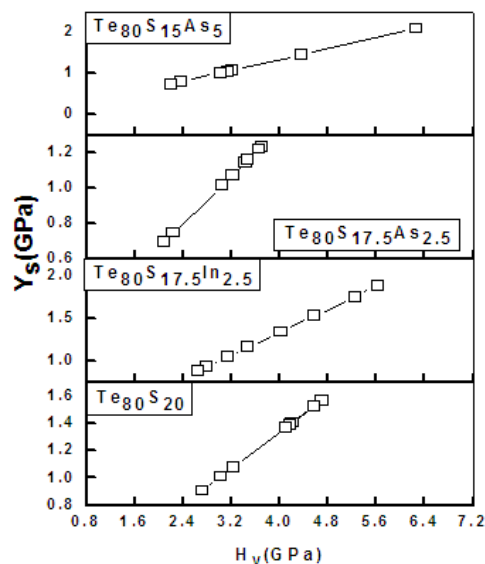


Fig [8] The brittleness (B) as a function of microhardness (H_v) of the chalcogenide system $Te_{80}S_{20-x}B_x$ [where $x=0, 2.5, 5$ B=In or AS] .

IV. Conclusion

The microhardness of samples of the system $Te_{80}S_{20-x}B_x$ [where $x=0, 2.5, 5$ B=In or AS] was increased with increasing of the applied test load. The addition of In or AS on the expense of S follow the same behavior. Mayer law proved that all samples of this system are soft and follow reverse indentation size effect (RISE). The indentation induced crack (IIC) model proves the generation of micro-cracks around the indentation points. This means that the mechanical resistance of each sample is increased as the applied test load increased. The behavior of the calculated elastic moduli confirm these results.

References

- [1]. Frerics, R.J., J. Opt. Soc. Am., 1953, vol. 43, p. 197.
- [2]. M.M.El-Zaidia, Z.H.El-Gohary, M.S.AboGhazala, G.M.Turky and E.A.Rebea, IOSR Journal of Electronics and Communication Engineering volume 13, Issue 5, 2018, pp54-59.
- [3]. M.M.El-Zaidia, Z.H.El-Gohary, M.S.AboGhazala, G.M.Turky and E.A.Rebea, IOSR Journal of Electronics and Communication Engineering volume 13, Issue 5, 2018, pp 49-53.
- [4]. G. E. Snopatin, V. S. Shiryayev, V. G. Plotnichenko, E. M. Dianov, and M. F. Churbanov, Inorganic Materials, 2009, Vol. 45, No. 13, pp. 1439–1460.
- [5]. F. Desevedavy et al, Applied Optics, Vol 48 (Issue 19): 3860 – 3865, (2009).
- [6]. K.Michel et al., Journal of Non-Crystalline Solids, Vol 326: 434 – 438, (2003).
- [7]. Pramesh Chandra1, Arvind K. Verma2, R. K. Shukla3 and Anchal Srivastava, International Journal of Advanced Scientific Research and Management, Vol. 2 Issue 8, Aug 2017.
- [8]. M. Popescu, J Optoelectron AdvMater 2005;7:2189–210.
- [9]. Amit Kumara, Mousa M.A. Imranb, Arvind Sharmaa, Neeraj Mehta, j m a t e r r e s t e c h n o l . 2 0 1 8 ; 7 (1) : 3 9 – 4 4 .
- [10]. Ningning Yin, Junfeng Xu, Fang'e Chang, Zengyun Jian, Chuanlei Gao, Infrared Physics and Technology 96 (2019) 361–365.
- [11]. L. Ćurkovi, M. Lali, S. Šoli, Kovove Mater. 47 (2009) 89–93.
- [12]. GONG, J.—WU, J.—GUAN, Z.: J. Eur. Ceram. Soc., 19, 1999, p. 2625.
- [13]. M.B. Turkoz, S. Nezir, O. Ozturk, E. Asikuzun, G. Yildirim, C. Terzioğlu, A. Varilci, by Lu addition. J. Mater. Sci.: Mater. Electron. 24, 2414–2421 (2013).
- [14]. Gergo Vassilev, Venceslav Vassilev*, and Lilia Aljihmani, P h y s . S t a t u s S o l i d i C 8, No. 11–12, 3115–3118 (2011).
- [15]. O. Ozturk1,2 · E. Asikuzun2,3,4 · A. T. Tasci1 · T. Gokcen1,5 · H. Ada6 · H. Koralay5 · S. Cavdar5, Journal of Materials Science: Materials in Electronics (2018) 29:3957–3966
- [16]. Suresh Sagadevan1,* , Shanmuga Sundaram Anandan, International Journal of Materials Engineering 2014, 4(2): 70-74.
- [17]. O. Ozturk, T. Gokcen, S. Cavdar, H. Koralay, A. Tasci, J. Therm. Anal. Calorim. 123, 1073–1082 (2016).

M.M.El-zaidia. " Mechanical Properties of Chalcogenide Optic Fiber Material Based Tellurium." IOSR Journal of Applied Physics (IOSR-JAP), vol. 11, no. 1, 2019, pp. 55-61